APPLICATION OF WAVELET ANALYSIS TO ULTRASONIC CHARACTERIZATION OF BONE

Wei Xu, Robert S. Siffert and Jonathan J. Kaufman

The Mount Sinai School of Medicine
One Gustave L. Levy Place, New York, NY 10029

Abstract

This paper investigates the application of time-frequency techniques to ultrasonic signals transmitted through bone to noninvasively determine bone density and strength. Ultrasonic transmission measurements are carried out on 3 samples of human vertebral trabecular bone, using a 1 MHz transducer pair. The data is processed using the wavelet transform according to Mallat's pyramid algorithm. The wavelet representation thus obtained is then cross-correlated with a wavelet representation of a reference signal to obtain the time-frequency representation associated with a particular bone sample. Results indicate that time-frequency methods may serve to accurately discriminate bone in various biophysical states. Further studies are under way to determine the best set of features associated with the time-frequency representation as well as the optimal means for processing the feature set, including neural networks.

Introduction

Recently, ultrasound has been proposed as a new technique for non-invasive clinical assessment of bone, an important component for managing metabolic bone diseases, especially osteoporosis [1]. Many studies have investigated the use of ultrasonic velocity and attenuation measurements to noninvasively characterize bone tissue. Results thus far have not demonstrated sufficiently high correlations with bone properties, in particular, bone density and strength. The goal of this study is to examine the use of time-frequency techniques and specifically the wavelet transform for processing ultrasonic signals to characterize the physical state of bone tissue.

Materials and Methods

Fresh lumbar vertebrae were acquired within three hours after extraction from human cadavers. In total, 3 vertebral bodies from 3 cadavers r anging in age from 30 to 93 years were used in this study. A two centimeter cylindrical core was cut from the central portion of each vertebral body using a drill with an attached drill corer. The cortical shell at both ends of the core was removed using a Buehler Isomet low-speed saw under constant irrigation, so that the specimen consisted only of vertebral trabecular bone. Bone samples were wrapped in plastic and frozen at -20°C until ultrasonic testing.

Each trabecular core was then ultrasonically tested along its superior-caudal axis to obtain the signal after propagating through the bone sample. The insertion methodology employed was as follows. The specimen was placed between two ultrasound transducers (Panametrics, Inc., #V303), each having a 1 MHz nominal center frequency and coaxially located on either side of the core. One transducer served to transmit an ultrasound pulse through a water bath and into one surface of the core, through the body of the core, out the opposite side, and through the water bath where the signal, denoted by $r_S(t)$, was detected by the other transducer acting as receiver. The received ultrasound waveform was collected on a digital oscilloscope card (Compuscope 220) at a 10 MHz sampling rate, and uploaded to a microcomputer for storage and subsequent off-line analysis. An ultrasound pulse that propagated through water only, denoted by $r_R(t)$, was also collected and served as a reference in the signal analysis.

The cores were then defatted by submersion in xylene for approximately 48 hours followed by a warm water rinse. The samples were then allowed to air dry for another 24 hours, at which time their weights were recorded. The apparent density was calculated by

1058-6393/95 $4.00

dividing the weight of each specimen by its total volume.

The ultrasound sample and reference signals, $r_S(t)$ and $r_R(t)$, respectively, were decomposed into a summation of wavelets at different scales [2] (the variable t is normalized to a nondimensional variable x, where $0 \le x < 1$). The wavelet expansion of $r_S(x)$ is expressed as [3]:

$$r_S(x) = a_0 \Phi(x) + a_1 W(x) + [a_2 a_3] \begin{bmatrix} W(2x) \\ W(2x-1) \end{bmatrix} +$$

$$[a_4 a_5 a_6 a_7] \begin{bmatrix} W(4x) \\ W(4x-1) \\ W(4x-2) \\ W(4x-3) \end{bmatrix} + \ldots + a_{2^j+k} W(2^j x - k) + \ldots \quad (1)$$

where the coefficients a_1, a_2, a_3, a_4,..., are the respective contributions of each wavelet function W(x) and $\Phi(x)$ is a scaling function. The coefficients are calculated according to:

$$a_{2^j+k} = 2^j \int_0^1 r_s(x) W(2^j x - k) dx \quad (2)$$

$$a_0 = \int_0^1 r_s(x) \Phi(x) dx \quad (3)$$

From Equ. (1), the ultrasonic signal can also be decomposed into the following representation:

$$r_s(x) = r_s^{(-1)} + r_s^{(0)} + r_s^{(1)} + r_s^{(2)} + \ldots + r_s^{(i)} + \ldots \quad (4)$$

$$r_s^{(i)}(x) = [a_{2^i}, \ldots, a_{2^{i+1}-1}] \begin{bmatrix} w(2^i x) \\ w(2^i x - 1) \\ \cdot \\ \cdot \\ \cdot \\ w(2^i x - 2^i + 1) \end{bmatrix} \quad (5)$$

$$r_s^{(-1)} = a_0 \Phi(x) \quad (6)$$

Equ. (5) is a decomposition of the bone signal, $r_S(x)$, into components at level i, i=-1,0,1,2,..., with each level centered at a distinct frequency. The original signal is the summation of all the separate wavelet levels. An identical processing technique is carried out for the reference waveform, $r_R(x)$.

In our studies, the specimen $r_S(t)$ and reference $r_R(t)$ signals are wavelet transformed by Mallat's pyramid algorithm using the D20 wavelet to achieve the necessary smoothness in the reconstruction [2,4]. The wavelet transform is implemented using Matlab (The Mathworks, Inc., South Natick, MA) [3] on signals with 512 data points. The resulting decomposition components have levels from i=-1 to i=8.

Finally, the time-frequency wavelet decomposition for each of the bone specimen signals was cross-correlated at each frequency level with the wavelet decomposition of the reference signal, which provides a measure of similarity between the specimen and reference signals for level i:

$$R_i(k) = \sum_n r_R^{(i)}(n) r_s^{(i)}(n+k) \quad (7)$$

where i = -1 to i=8. The cross-correlation function $R_i(k)$ was plotted for each of the three bone sample signals, as a function of time (k) and frequency (i).

Results

Figures 1a-1c display ultrasonic signals $r_S(t)$ for the three bone samples having densities of 0.12, 0.22, and 0.29 g/cm^3, respectively. The signal associated with the middle range density value (i.e., Fig. 1b) may be seen to consist of at least two distinct components, namely, a low frequency early time component and a higher frequency later time component. Figure 1d displays the reference waveform after propagation through water only. Note that it is very similar to Fig. 1a, the signal associated with the lowest density bone sample. Figures 2a-2c display the three-dimensional perspective plots for the time frequency cross-correlation functions of the bone sample signals. As may be seen, the three-dimensional perspective graphs demonstrate significant qualitative differences in both frequency and time.

Discussion

Wavelet transform techniques are recognized as a useful tool for time frequency representation, which preserves both time and frequency information, unlike Fourier analysis in which the location of a particular frequency on the time axis will be lost. We have presented here preliminary results of applying time frequency techniques to ultrasonic signals in human trabecular bone. The work is motivated by the fact that fluid filled porous structures such as bone may have associated with them both slow and fast modes of wave propagation [5-7]. This apparently gives rise to the variation in time observed of the arrival of acoustic wave components. The data presented appear to indicate that wavelet techniques may have useful application in the noninvasive identification of bone state. As may be seen in Figs. 2a-2c, the time frequency representation associated with the least dense bone has little signal energy associated with the earliest time of arrival. In contrast, the most dense bone has significant low-frequency and early time signal energy.

Further work is currently being conducted to identify the optimal set of features based on the time-frequency representation, and to apply various pattern recognition techniques, including regression and neural network analyses, in an effort to accurately estimate bone density and strength from ultrasonic measurements.

References

[1] JJ Kaufman and TE Einhorn. Ultrasonic Assessment of Bone: A Review. *Journal of Bone and Mineral Research, Vol. 8*, Number 5, pp. 517-525, 1993.

[2] I Daubechies. "Orthonormal Bases of Compactly Supported Wavelets," *Communication on Pure and Applied Mathematics, V.41*, pp. 909-996, 1988.

[3] DE Newland. *An Introduction to Random Vibrations, Spectral and Wavelet Analysis*, Longman Scientific, England, 3rd Edition, 1993.

[4] SG Mallat. *A theory for Multiresolution Signal Decomposition: the Wavelet Representation*, IEEE Trans. PAMI-11, No.7, pp. 674-693, 1989.

[5] MA Biot. " *JASA*, 28, p. 168, 1956.

[6] DL Johnson. "Recent developments in the acoustic properties of porous media," in *Frontiers in Physical Acoustics*, pp. 255-290, 1986.

[7] JL Williams. "Ultrasonic wave propagation in cancellous and cortical bone: prediction of some experimental results by Biot's theory," *JASA*, 91(2), pp. 1106-1112, 1992.

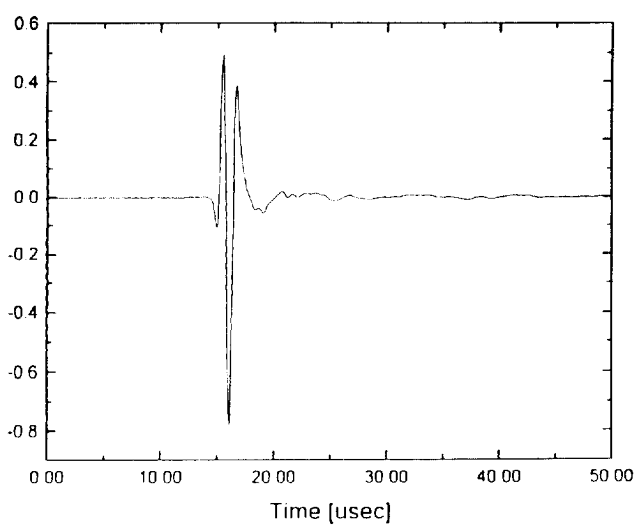

Fig. 1a: Ultrasonic signal for bone sample of density 0.12 g/cm^2.

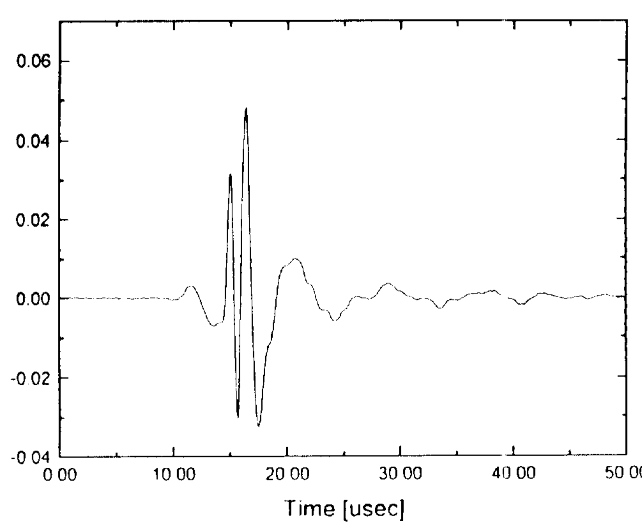

Fig. 1b: Ultrasonic signal for bone sample of density 0.22 g/cm^2.

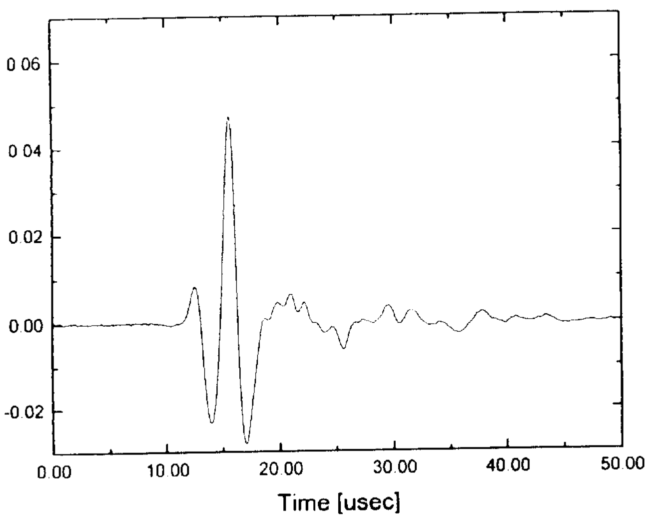

Fig. 1c: Ultrasonic signal for bone sample of density 0.29 g/cm^2.

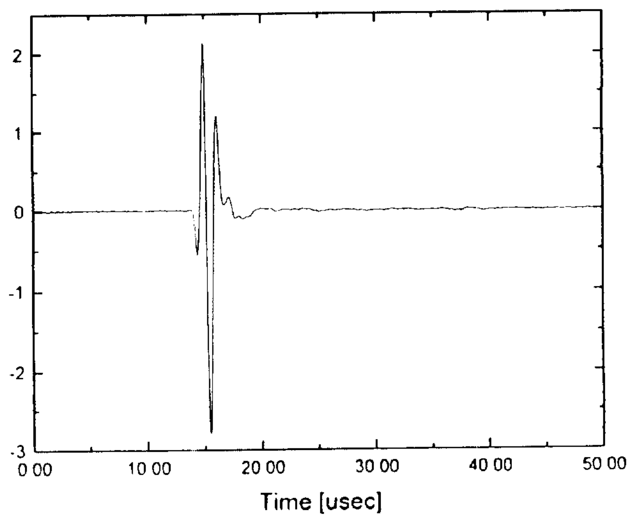

Fig. 1d: Ultrasonic reference signal (water path only).

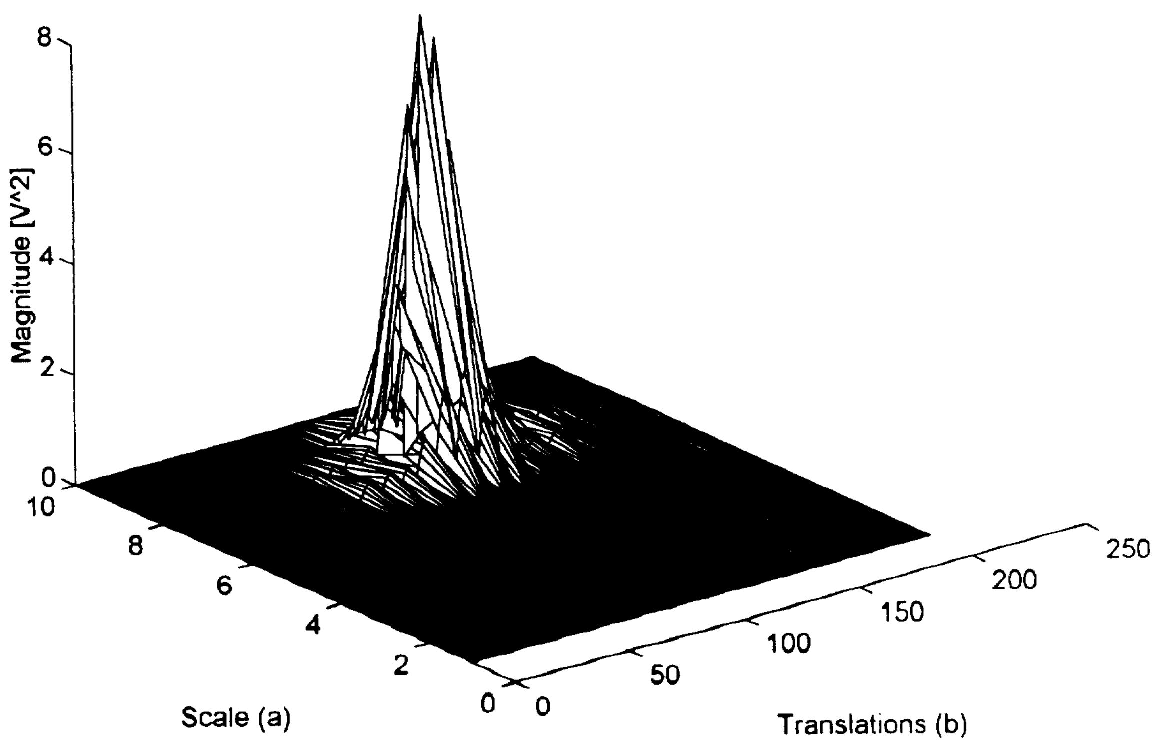

Fig. 2a: Time-frequency representation for ultrasonic signal in Fig. 1a.

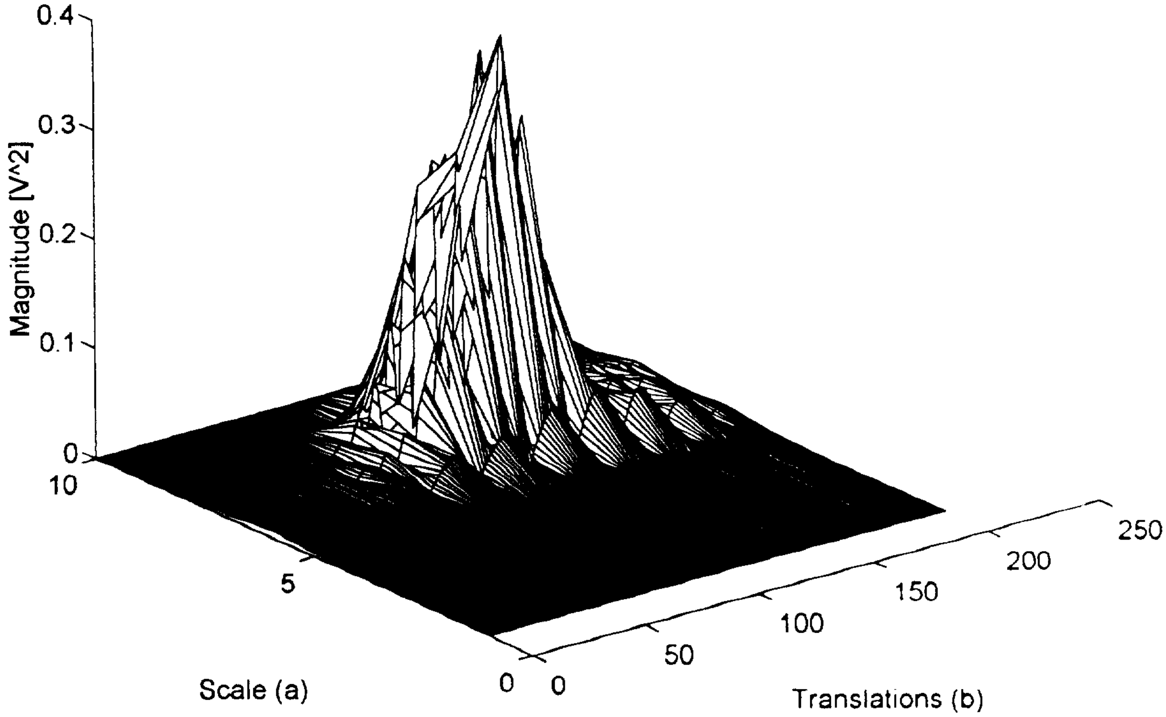

Fig. 2b: Time-frequency representation for ultrasonic signal in Fig. 1b.

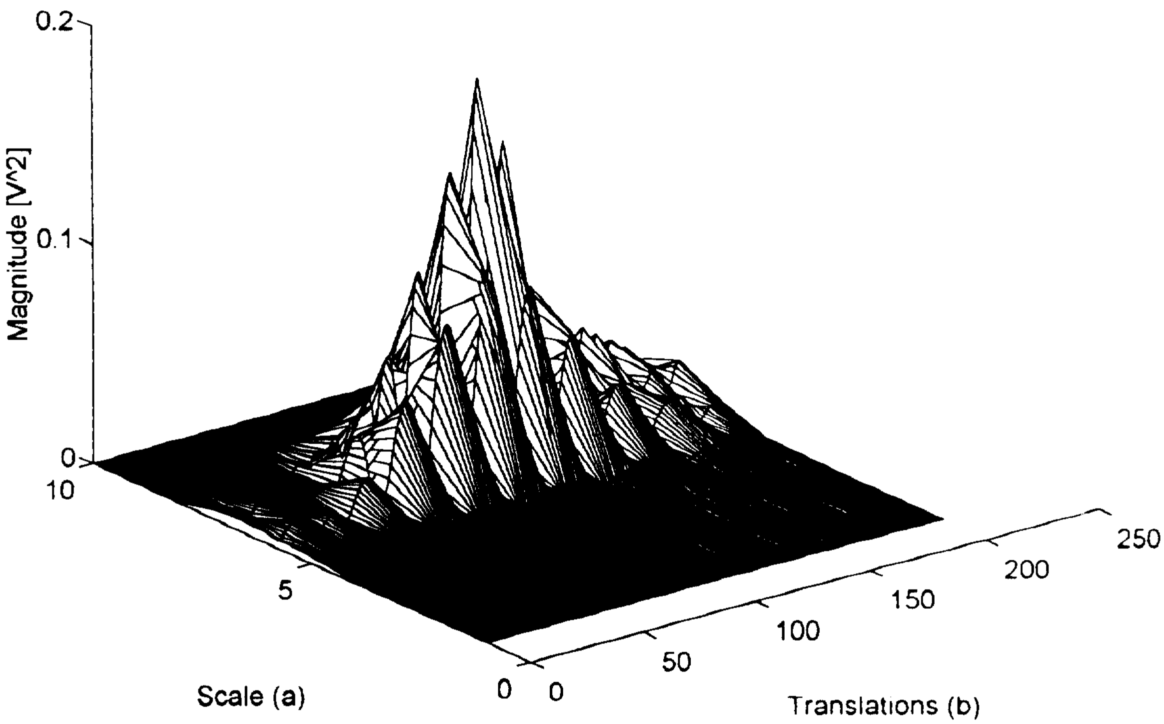

Fig. 2c: Time-frequency representation for ultrasonic signal in Fig. 1c.